Drug Mimetic Organogelators for the Control of Concomitant Crystallization of Barbital and Thalidomide

Basanta Saikia,[a] Matthew T. Mulvee,[b] Ivan Torres Moya,[c] Bipul Sarma,[a] Jonathan W. Steed[b]**

[a] Department of Chemical Sciences, Tezpur University, Napaam-784028, Assam, India

[b] Department of Chemistry, Durham University, South Road, Durham, DH1 3LE, UK

[c] Department of Organic Chemistry, University of Castilla La Mancha, 13071 Ciudad Real, Spain.

E-mail: [a] bcsarma@tezu.ernet.in, [b] jon.steed@durham.ac.uk

Keywords: Concomitant polymorphism, Organogelators, Bis(urea), Gel phase crystallization, Barbiturates

Abstract

A strategic approach to control the polymorphism of two related drugs by introducing a drug-mimetic imide functional group into the molecular weight organogelator structure is presented. This was achieved with novel aminoglutethimide-derived bis(urea) organogelators designed to form gels that act as targeted crystallization media for (±)-thalidomide and barbital. The organogelators prevent concomitant crystallization, a serious issue for drug formulation and development. This work demonstrates the potential to control concomitant crystallization with rationally designed supramolecular gelators.

Introduction

Supramolecular gels are formed through the self-assembly of gelators (typically at low concentrations *i.e.* <2% by mass) into filaments which entangle and branch to form a three-dimensional network that immobilizes the solvent to produce a viscoelastic material.[1–5] These gelators can be relatively straightforward to synthesize and functionalize, with potential applications in catalysis, biomedical research, drug delivery and pharmaceutical crystallization.[6–11] Bis(urea) gelators, in particular, can be synthetically modified to design gelators with desired functionalities and specific properties while retaining their gel-forming ability.[12] Generally, bis(urea) gels are thermally reversible as they are formed through reversible non-covalent interactions and their gelation behavior can be manipulated by altering the experimental conditions.[2,13–15] Furthermore, the prevention of convection effects, reduced solvent evaporation rate and the possibility of designing drug-specific binding functionality, means that supramolecular gels are emerging as effective media for pharmaceutical crystallization.[11,16,17]

Drug solid form screening, solid form control and crystal morphology are of key industrial significance.[18,19] Crystal form control has vital importance in the pharmaceutical development process as different crystal structures (polymorphs) or solvated forms (solvates) of the same drug exhibit different physiochemical properties such as solubility, tabletability, melting behavior, hydration stability, bulk density and bioavailability, which eventually impact on the overall drug efficacy.[18] In addition, factors like crystal morphology and particle size also need careful attention as they can influence the drug physiochemical, formulation and processing properties.[20] Moreover, a thorough understanding of the solid forms landscape can represent intellectual property opportunities.[21] Nucleation events and crystal growth can be guided at interfaces by molecular recognition. Crystallization using heterogeneous surfaces such as a self-assembled monolayer (SAM),[19] or a polymer additive and techniques like laser-induced crystallization,[22] are also being

incorporated into pharmaceutical screening and solid form control and discovery methods.[23] New crystallization methods such as nanoconfinement, nanodroplet crystallization,[24] the use of tailored additives[25,26] and careful temperature control[27] are significantly expanding solid form landscapes. Bora *et al.* recently reported that crystallization on functionalized SAM surface could effectively control concomitant nucleation of flexible molecules.[19]

Recent work has demonstrated the feasibility of gel-phase crystallization to control crystal size, morphology and polymorphic outcome.[11,16,28,29] It has been proposed that the gel fibers can act as a surface for templated nucleation of active pharmaceutical ingredients (APIs). Different solid-state crystal forms (polymorphs) can differ in lattice energy by only a few kJ mol^{-1} [30,31] and so the presence of the gel fiber surface can bias the system towards the crystallization of a particular form.[32] Depending on the gel-solute interactions, gels offer the possibility of obtaining new forms or metastable solid forms that are not be obtainable from the conventional crystallization methods.[11,17] Functionalized gels can offer potential alternate nucleation sites and hence can influence the crystallization outcome. Polymorphic control of the highly polymorphic molecule ROY has been demonstrated by utilizing a rationally designed organogel as the crystallization medium.[16] Other modifications of crystal properties such as size, morphology, and change in polymorphism in gel phase crystallization have been reported.[11,16,17,29,33]

While often the discovery of gelators is serendipitous, bis(urea)s are prone to form gels in the presence of a wide variety of terminal substituents as they often aggregate *via* one-dimensional hydrogen bonding to form highly anisotropic morphologies that are commonly linked to gelation.[4,12] As the urea groups are expected to be involved in urea α-tape like hydrogen bonding it is possible to append drug-mimetic functional groups at the periphery of the gelator that are available to interact with the API solute and hence influence its crystallization.

Despite its notorious history, (±)-thalidomide (THL) has attracted considerable clinical interest in recent years due to its unique pharmacological effect against several diseases, especially cancer.[34] Racemic THL has two known solid forms, termed α and β.[35] Barbital (BAR) was the first commercially available barbiturate and is a well-known sedative.[36] It is highly polymorphic with six known non-solvated forms.[36] Crystal structures of three polymorphs of BAR *i.e.* forms I, III and V have been reported, which exhibit packing polymorphism, and are known to crystallize concomitantly (Scheme 1).[36,37] Concomitant polymorphism involves the crystallization of different forms, from the same crystallization batch and it is common when the crystal packing energy differences between forms are relatively insignificant.[19,38,39] However, formulation of a pure single form of a drug is crucial in the pharmaceutical industry since varying amounts of different polymorphs can give rise to an inconsistent product profile and performance. Therefore attaining control over concomitant polymorphism as observed for BAR is essential from its efficacy and formulation point of view.[40]

In this work, we have designed three new bis(urea)-based low molecular weight gelator (LMWG) bearing the drug-mimetic imide group that occurs in important drug classes such as barbiturates and thalidomide and its analogs to act as a potential site of interaction with the target APIs (Scheme 2). We show that these targeted gelators achieve control over the concomitant polymorphism of BAR and influence the outcome of THL crystallizations.

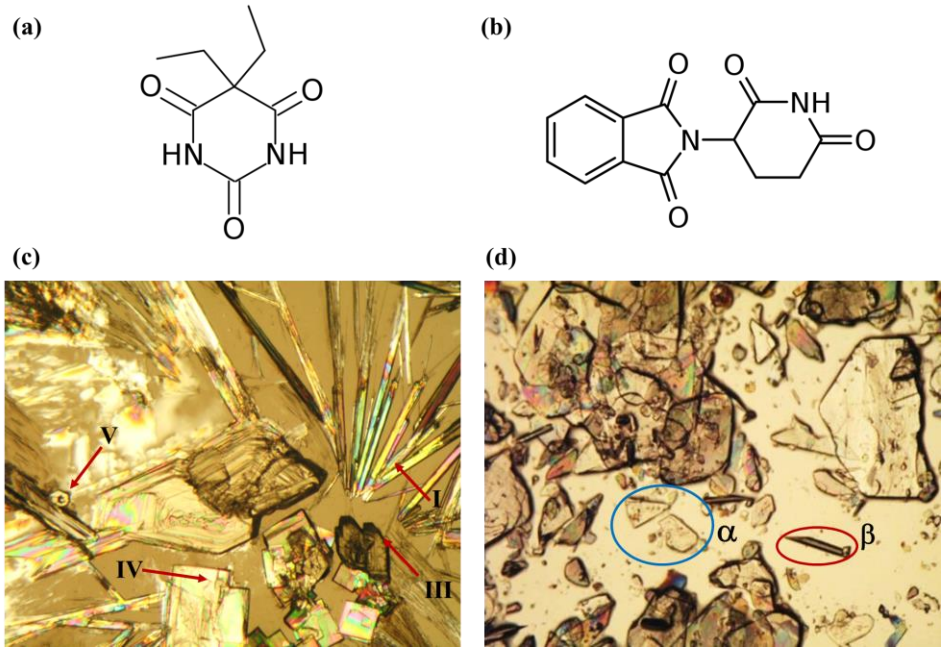

Scheme 1 Chemical structures of APIs (a) barbital (BAR) and (b) (±)-thalidomide (THL); concomitant polymorphism from solution crystallization of (c) BAR from cyclohexanone and (d) THL from nitromethane. Needle *β* form (red circle) and plate-shaped *α* form (blue circle) of THL.

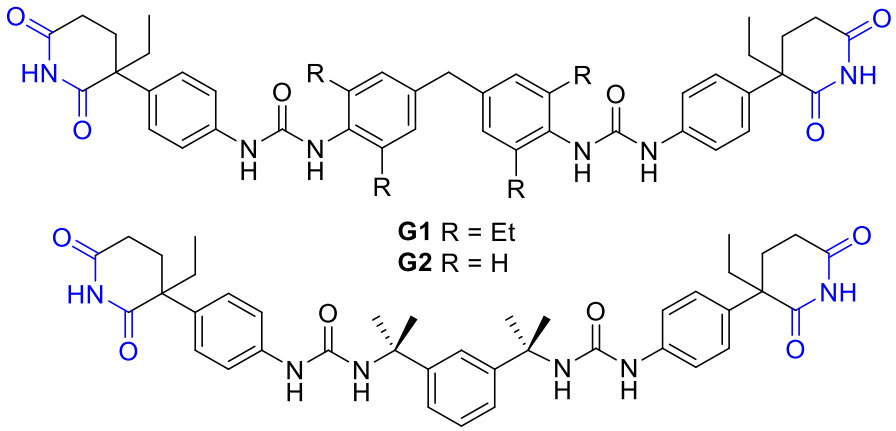

Scheme 2 Design of drug mimetic gelators **G1**–**3**, with the imide group shown in blue.

Results and Discussion

Synthesis

The three gelators (**G1** – **G3)** were synthesized in good yield using the commercially available (±)-aminoglutethimide as the precursor and the appropriate diisocyanate (see Electronic Supporting Information, Schemes S1 – S3). The gelators were characterized by nuclear magnetic resonance (NMR) spectroscopy, Fourier-transform infrared (FTIR) spectroscopy, mass spectrometry and elemental analysis (see ESI).

Gel screening and Characterization

Gel screening of **G1, G2 G3** was carried out using a wide range of solvents and solvent combinations at 2 % (w/v) (Table 1). Samples were dissolved with gentle heating and sonication until full dissolution. Gel formation was typically observed upon cooling to room temperature within a few minutes though in some cases gelation took several hours. Gel formation was assessed qualitatively by simple inversion of the sample vial. Gelator **G1** forms gels in 13 of the 29 solvents and solvent combinations tested including some alcohols, cyclic ketones, 1,4-dioxane and nitro compounds (See ESI Figure S4).

The low solubility of gelator **G1** prevents the formation of gels in most alcoholic solvents such as methanol and 1-propanol. The addition of a few drops of DMSO readily dissolved the gelator with further heating so that it forms gels in all the alcoholic solvents tested upon cooling. The critical gelation concentration (CGC) for **G1** is typically 1.7 – 2 % (w/v) for alcoholic solvents, while in the case of nitrobenzene, cyclohexanone, cyclopentanone, 1,4-dioxane, tetrahydrofuran a lower CGC of 0.8 – 1 % (w/v) was observed. While **G1** is an effective gelator, **G2** and **G3** form gels in only in two or three different solvents or solvent mixtures (Table 1). Gelator **G2** forms gels in nitrobenzene and a 3:1 mixture of ethanol and cyclohexane (see ESI Figure S4b) with CGC of 0.8 and 0.9 % (w/v), respectively. **G3** gels nitrobenzene, nitromethane and a 2:1 toluene/ethyl

acetate mixture (see ESI Figure S4c) with a CGC of 0.8 % (w/v) in each case. All gels were either translucent or opaque and became more opaque over time. This is commonly attributed to fibers laterally associating to form larger bundles, which scatter light more, thus appearing more opaque.[41,42] FT-IR analysis of the gels demonstrated a lowering of the IR frequency for carboxamide peak (~1692 cm^{-1}) for the gels, which we attribute to intermolecular hydrogen bonding between the gelator molecules (ESI Figure S5).

Table 1 Gel screening results for **G1**, **G2** and **G3**, all at 2% (w/v).

Solvent	**G1**	**G2**	**G3**
1,2,4-trichlorobenzene	P	S	S
2-propanol	PG	PG	S
Acetone	P	S	S
Ethanol	G	PG	PG
Methanol	PG	PG	PG
Methanol+ DMSO	G	PG	PG
1-Pentanol	G	PG	PG
1,4-Butanediol	G	PG	PG
1-Propanol	PG	PG	PG
1-Propanol+ DMSO	G	PG	PG
1-Butanol	G	S	PG
2-Butanol	PG	IS	PG
2-Butanol+ DMSO	G	S	PG
Benzyl Alcohol	PG	S	S
Chloroform	IS	IS	IS
Dimethyl sulfoxide	S	S	S

Dimethylformamide	S	S	S
Ethyl Acetate	IS	IS	S
Nitrobenzene	G	G	G
Nitromethane	G*	PG	G
1,4-Dioxane	G	S	S
Tetrahydrofuran	G	S	S
Cyclohexanone	G	S	P
Cyclopentanone	G	P	P
Toluene	P	P	S
H_2O	P	S	S
EtOH: Cyclohexane (3:1)	PG	G	PG
Toluene: Ethyl acetate (2:1)	PG	PG	G

P= Precipitate, G= Gel, PG= Partial Gel, I= Insoluble with heating. * Very soft gel

The sol phase transition temperature, T_{gel}, was recorded by heating the gels and recording the temperature at which a small ball bearing fell through the sample, indicating disruption of the gel network.[43] Gels formed with **G1** were found to be generally quite stable with a T_{gel} of 97 °C at a concentration of 2% (w/v) for cyclohexanone (see ESI, Table S1). The gel of **G3** in nitromethane has a much lower T_{gel} of 45 °C at 2 % (w/v). In nitrobenzene and a mixture of toluene/ethyl acetate (2:1) the T_{gel} values for **G3** are 101 and 83 °C, respectively. The latter value is above the 77 °C boiling point of ethyl acetate and was evaluated in a sealed container. This relatively high T_{gel} suggests that gels of **G3** may be relatively robust.

Representative gels were characterized using oscillatory rheology. In all cases, the storage modulus (G') was at least an order of magnitude greater than the loss modulus (G''), indicative of the solid-like nature of the materials (Figure 1).[44,45] The mechanical properties of the gels were

relatively insensitive to the oscillation frequency, with G' higher than G'' in all cases, and they remain almost constant over the entire angular frequency range (ESI Figure S7), again typical behavior for supramolecular gels. Scanning electron microscopy (SEM) was used to image the morphology of the xerogels formed from **G1**, **G2** and **G3** a highly entangled network as observed for all samples (Figure 1b). The SEM sample of **G1** is obtained from drying a 2% (w/v %) gel in ethanol and shows a helical twisted morphology (Figure 1bi). A cylindrical ribbon type morphology is observed for a 1 % (w/v %) xerogel of **G2** obtained from nitrobenzene (Figure 1bii). A dense network of helical morphology is observed for 1 % (w/v %) xerogel of **G3** in nitromethane (Figure 1biii).

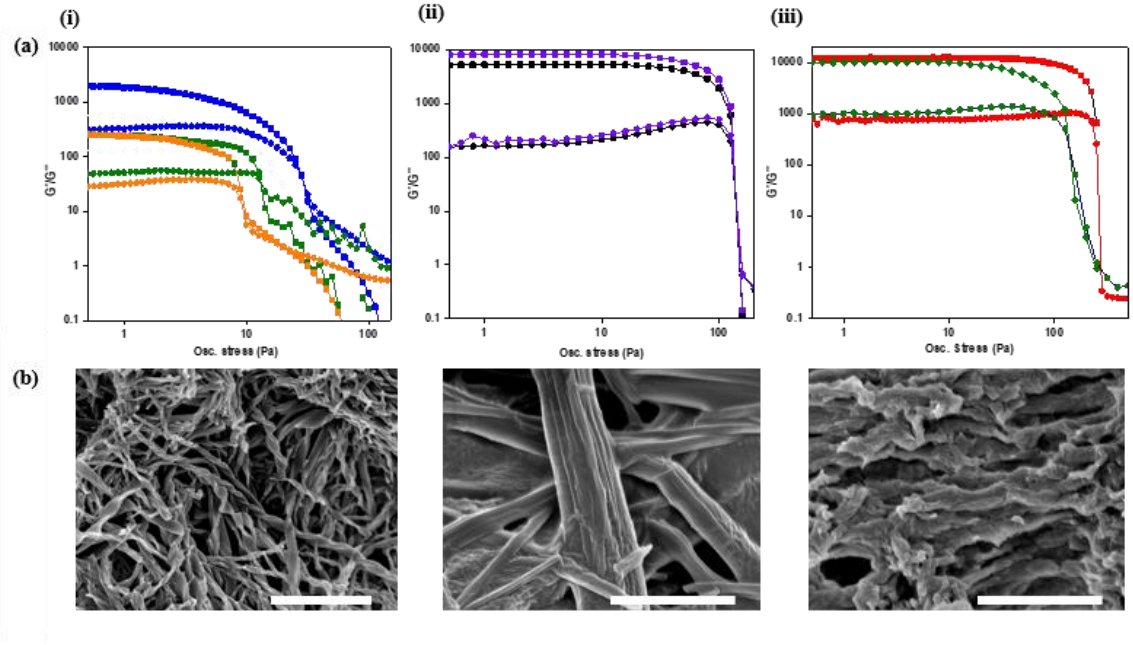

Figure 1 (a) Oscillatory stress sweeps at a constant frequency (1 Hz) (i) **G1**, (ii) **G2** and (iii) **G3**. (i) Cyclohexane (blue), nitrobenzene (green), butanol (orange); (ii) ethanol: cyclohexane 1% (w/v) (black), 2 % (w/v) (purple); (iii) nitromethane (red), toluene: ethyl acetate (2:1) (green). In all cases ■ refer to G′ (elastic moduli) and ● refer to G″ (viscous moduli). (b) SEM images of the xerogels (i) **G1**, (ii) **G2** and (iii) **G3** demonstrates the fibrous nature of the gels. (Scale bar: 2 μm)

Crystallization of Barbital

The UNI force-field introduced by Gavezzotti and Filippini[46,47] and implemented in the Cambridge Crystallographic Data Centre Mercury package (Mercury 4.2.0)[48] was used to calculate the relative packing energy of the BAR polymorphic forms based on the single-crystal structures (DETBA01-12) deposited in the Cambridge Structural Database.[49] The packing energies are comparable with packing energy –114.9, –118.2 and –119.5 kJ mol^{-1} for polymorphs I, III and V, respectively. These similar packing energies are consistent with the observation of concomitant polymorphism.

Table 2 Comparison of crystallization outcome from solution and gel crystallization of barbital.

Solvent	**Solvent Crystallization**	**G1**	**G2**	**G3**
Ethanol	I, III, IV, V	III (prism), V	No gel	No gel
1-Butanol	I, III, V	III (rod)	No gel	No gel
1,4-Butane-diol	I, III, V	III (prism)	No gel	No gel
1-Pentanol	I, III, IV, V	III (prism)	No gel	No gel
Nitrobenzene	III	III	III	III
Nitromethane	III (needle)	III (prism)	No gel	Gel Unstable
Cyclohexanone	I, III, IV, V	III (prism)	No gel	No gel
Toluene/ethyl acetate (2:1)	III and V	No gel	III (prism)	No gel
EtOH/cyclohexane (3:1)	III and V	No gel	No gel	III (prism)

Solution crystallizations were performed by slow evaporation in a sealed vial with pinhole openings at room temperature. Crystallizations of barbital in the gels were carried out in parallel to solution crystallization, at 10% w/v.

The tendency of BAR to crystallize multiple forms concomitantly is well known and occurs in many solvents (Table 2).[36,37] Similarly subliming BAR between 100 and 120°C results in the concomitant crystallization of forms I, IV, V and III.[36] MacDonald *et al*. employed chemically modified surfaces in microfluidic channels to control the nucleation of barbital polymorphs, however, they were not able to control selectivity between forms I, III and IV at the surface of SAMs.[37] Gel phase crystallizations of BAR were carried out in parallel to solution crystallization, typically at 10% w/v and crystals typically formed in 3-4 days (see Experimental for details). The crystals that were obtained from control solution crystallization from alcoholic solvents gave rise to concomitant crystallization of polymorphs I, III, IV and V of BAR which were identified by optical microscopy, single-crystal unit cell determination for at least five crystals, PXRD, DSC and FT-IR analysis.[36] Form I and III proved to be more abundant by solvent crystallization and occurred along with forms V and IV. However, form IV transform to Form I within 30 minutes outside solvent at room temperature and demonstrated by FT-IR analysis (ESI, Figure S8). Under the same experimental condition *i.e.* 100 mg/mL of barbital, gels of **G1** in 1-butanol (1.8 w/v %), 1-pentanol (1.8 w/v %), and 1,4-butanediol (1.8 w/v %), produced only the kinetic form III of BAR. However, in the case of ethanol (1.7 w/v %) trace amount of crystals of another kinetic form, form V was also observed along with polymorph III. In the case of nitrobenzene, no differences between crystals obtained from the solution and gel phase crystallization were observed. This is not surprising since the kinetic form is already favored in nitrobenzene. The solution crystallization of BAR from nitromethane (10 w/v %) resulted in dense needle-shaped crystals (Figure 3aiii). These crystals were analyzed by FTIR spectroscopy and unit cell determination and were found to be a concomitant mixture of polymorphs III and V. However, nitromethane gels of **G1** (2 w/v %) produced large prism-shaped crystals of polymorph III without the concomitant presence of Form

V. Thus, in contrast to solution crystallization methods, gel phase crystallization of BAR using the gelator **G1** exhibits high selectivity for the kinetic form III polymorph. This selectivity is also observed for gels formed using **G2** and **G3** in two different solvents implying that the common imide on all the gelators plays major role in control the crystallization outcome. It is possible that the interaction of the drug molecules with the gel fiber surface might increase the nucleation rate of the kinetic form and thereby suppresses the nucleation of competing forms. A comparison between gel phase and solution phase crystallization outcomes is shown in Figure 3. In the presence of gelator in the gel state can alter the crystallization behavior of barbital and thereby prevent the concomitant crystallization and confirmed the observations from PXRD, DSC, FT-IR and SCXRD. These observations were further verified by conducting additional gel phase crystallizations using previously reported gelators that do not contain the imide functionality; **G4** contains nitro aryl groups,[16] and **G5** a salt gelator bearing carboxylate groups (Figure 2).[50] All crystallizations in these gels failed to prevent concomitant polymorphism. This indicates that it the imide functionality of the mimic gelators rather than the growth in a viscous gel network that prevents concomitant crystallization either enhancing nucleation of Form III or, more likely, suppressing nucleation of the other forms. Furthermore, quantitative analysis of the intermolecular interactions for the different forms of BAR i.*e.* I, III and V were performed using Hirshfeld surfaces and represented as 2D fingerprint plots (ESI Figure S10).[51] Significant differences were observed for the different forms. Notably, the higher contribution of the O···H interactions in form III (45%) compared to Form I and V (40.8% and 40.1%, respectively). Thus, it speculated that the polar end groups of the mimetic gelators may be able to interact with the nuclei of Form III more favorably and promote the growth due to a local supersaturation of this form over Form I or V.[52]

However, crystal growth mechanisms and the link between nuclei ordering and the final crystal structure are not well understood, and is beyond the scope of this work.

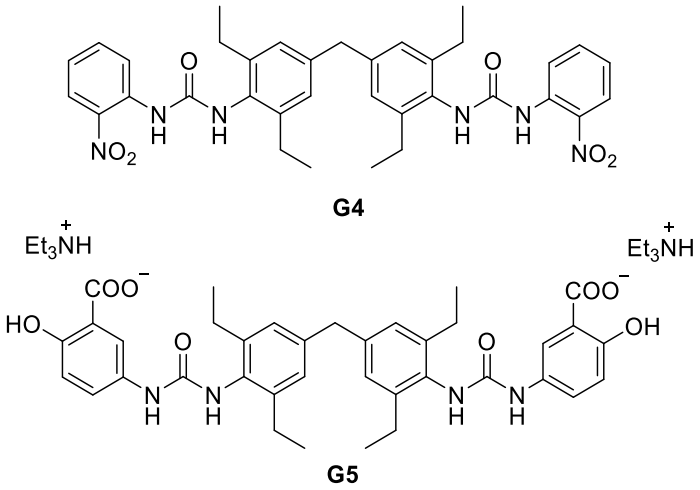

Figure 2 Chemical structures of control gelators **G4** and **G5** for the crystallization of BAR.

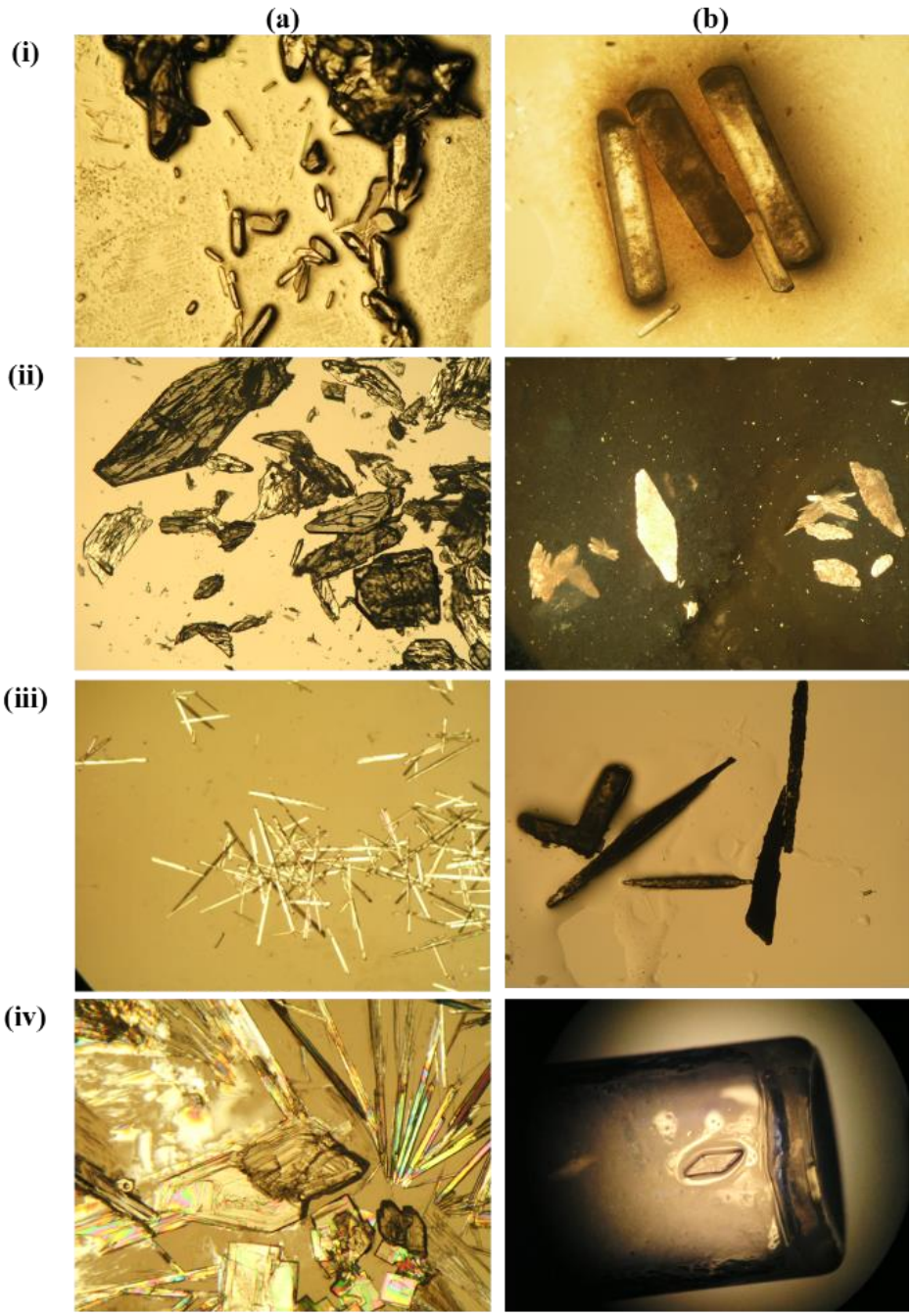

Figure 3 Photos of BAR crystals produced from (a) solution crystallizations and (b) **G1** gel phase crystallizations in (i) 1-butanol, (ii) ethanol, and (iii) nitromethane and (iv) cyclohexanone, respectively.

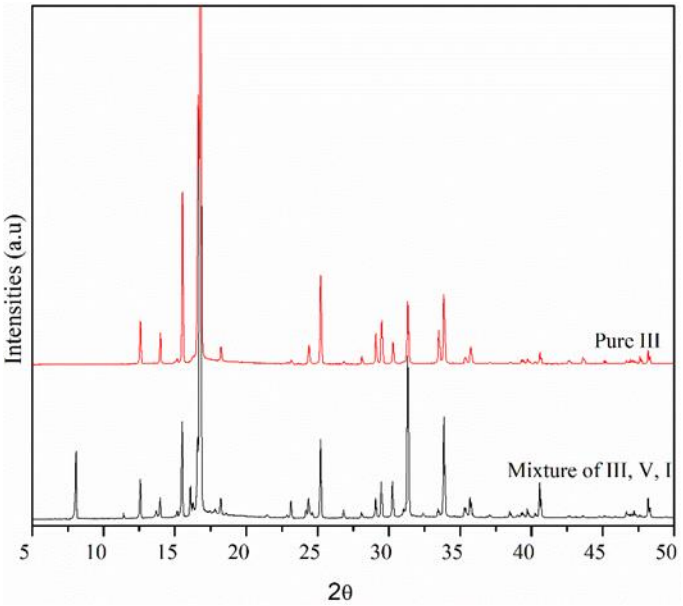

Figure 4 PXRD patterns of BAR only polymorph III obtained inside the gel **G1** in 1-butanol and the mixture of polymorphs obtained from solution crystallization from 1-butanol

Thalidomide Crystallization

(±)Thalidomide has very low solubility in most organic solvents and is practically insoluble in alcohols. So, the crystallization of this drug was restricted to nitromethane, 1,4-dioxane, nitrobenzene and cyclohexanone. To our knowledge concomitant polymorphism of THL has not previously been documented in the literature. Packing energy calculations were undertaken using Mercury 4.2.0[48] for the crystal structures (THALID11-12) deposited in the Cambridge Structural Database and demonstrated comparable packing energies for polymorphs α (–150.6 kJ mol^{-1}) and β (–156.9 kJ mol^{-1}). Interestingly, the two polymorphs crystallize concomitantly upon solution crystallization from nitromethane at concentration 20 mg/mL (Figure 5a). From the solution crystallization in nitromethane, large plate and small needle-shaped crystals were observed. The plate and needle-shaped crystals were characterized by FT-IR spectroscopy, PXRD, and unit cell parameter determination and confirmed as the α and β forms, respectively.[35] The polymorphs can be easily distinguished by comparison of their FT-IR spectra in which the α polymorph exhibits

N-H stretching modes at 3193 and 3098 cm^{-1} while the β polymorph exhibits peaks at 3278 and 3111 cm^{-1} as shown in Figure 6. Crystallization of THL in nitromethane **G1** gels prevents this concomitant crystallization, such that only kinetic form α is formed (Figure 5b). To confirm the phase purity of the crystals obtained inside the gel the PXRD pattern was compared with that simulated from the single-crystal structure and they were found to be in an exact match (see ESI Figure S9).

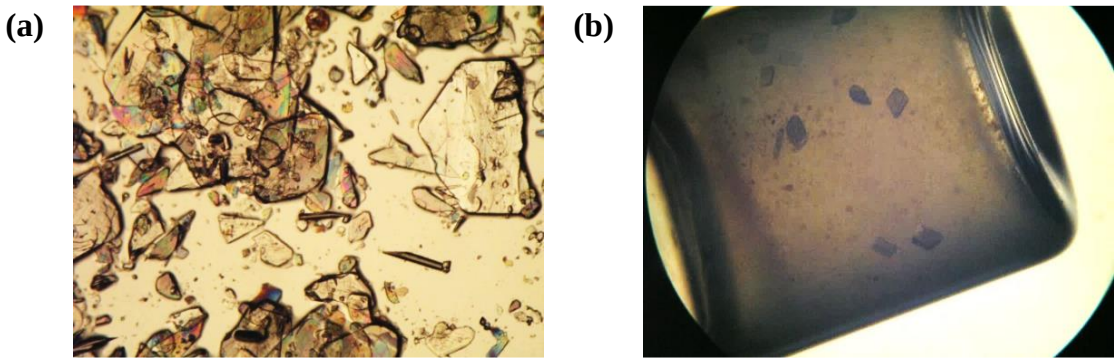

Figure 5 (a) Concomitant crystals plate (α) and needle (β) of THL obtained from solvent evaporation in nitromethane and (b) crystals of only α grown inside the **G1** gel in nitromethane.

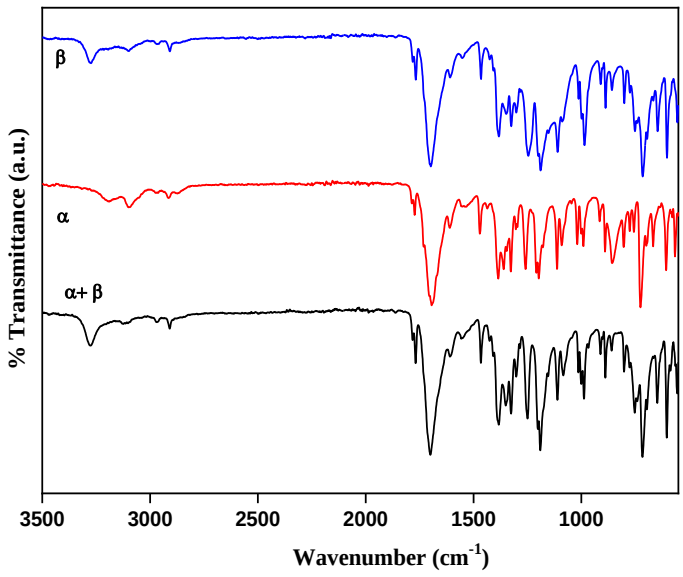

Figure 6 FT-IR spectra comparisons of THL polymorphs α grown inside the gel (red) and concomitant crystals of α and β of THL obtained from solvent evaporation (black) in nitromethane.

The FT-IR spectrum of the β polymorph of THL was obtained by manually separating the crystals (blue).

Under comparable conditions no substantial changes in polymorphic outcome were observed between gel phase (**G1**) and solution phase crystallization by slow cooling in nitrobenzene, 1,4-dioxane and cyclohexanone. However, the gel phase method resulted in a habit change with comparatively larger crystals being formed in the gels compared to solution crystallization in 1,4-dioxane (Table 3).

Table 3 Comparison of crystallization outcome from solution and Gel crystallization of THL

Solvent	**Crystal forms in pure solvent**	**Crystal forms from gel G1**	**Crystal forms from gel G2**	**Crystal forms from G3 gel**
Nitromethane	α and β	α	No gel	Gel not stable
1,4-dioxane	α	α*	No gel	No gel
Cyclohexanone	No crystals	α*	No gel	No gel
Nitrobenzene	No crystals	α†	α†	No crystals

*large needles, †very small crystals

Conclusions

Three new bis(urea) based drug mimetic molecular organogelators were synthesized by the reaction of (±)aminoglutethimide with different diisocyanates. Rheological analysis and SEM images confirm that all three form supramolecular gels with the ethyl-substituted diphenylmethane gelator **G1** being by far the most versatile, consistent with previous.[4,17] The gelators were used as a crystallization media for crystallization of imide containing drugs barbital and (±)-thalidomide. While solution crystallization of BAR in many solvents gave rise to concomitant mixtures, gel phase crystallization using these novel gelators exhibited high selectivity towards the kinetic form

III polymorph of barbital. Similarly, in the case of THL, gels of **G1** selectively crystallize the kinetic α form while concomitant mixtures of forms α and β were obtained using solution crystallization methods. It is speculated that the local order of the gel fibers may provide a preferred nucleation site for certain forms and sufficiently favor their crystallization to avoid concomitant crystallization. The use of non-mimetic gelators did not prevent concomitant crystallizations. This indicates that the viscous gel media is not primarily responsible for favoring the kinetic forms. Thus, the use of drug-mimetic gelators is necessary to prevent the concomitant crystallization of BAR and THL. This work demonstrates a promising route to preventing concomitant crystallization in other systems.

Experimental

Materials and Methods

All the chemicals used were brought from standard commercial sources and were used as such without further purification. (±)-aminoglutethimide was purchased from TCI. The isocyanates were purchased from Sigma Aldrich. All solvents of HPLC grade, triethylamine, and chloroform used in the experiments were purchased from Merck.

FTIR spectra of the gelators and the obtained polymorphic form of the drug BAR and THL were recorded in the frequency range of 600–4000 cm^{-1} in a Perkin Elmer Spectrum 100 ATR instrument. Powder diffraction patterns were recorded on a PANalytical Empyrean diffractometer using Cu Kα radiation (λ = 1.54Å), tube voltage of 40kV and 40mA current. Intensities were measured from 5° to 50° 2θ with 0.04 rad. Soller silts and an incident beam divergent slit of 1/8°, antiscatter slit of 1/4° and diffracted beam anti-scatter slit of 7.5mm (PIXcel). All NMR spectra were recorded using a Varian Mercury 400 (^{1}H: 400 MHz; ^{13}C: 100 MHz) spectrometer at room

296 temperature using deuterated solvent DMSO-d_6. Mass spectra of the compounds were collected
297 using a Thermo-Finnigan LTQ FT mass spectrophotometer. Samples were dissolved in methanol
298 and mass spectra were collected in positive electron spray (ES) mode in the case of **G2** and **G3**,
299 whereas matrix-assisted laser desorption/ionization (MALDI) was used for **G1**. Elemental analysis
300 is performed by using an Exeter Analytical Inc. CE-400 elemental analyzer. Typical sample size
301 5-7 mg was used to calculate the C, H and N percentage of the prepared compounds. Rheological
302 experiments were performed using advanced rheometer AR 2000 from TA Instruments. The
303 rheometer was equipped with a chiller (Julabo C). Stainless steel 20 mm plain plate geometry was
304 used to perform the experiments. Samples of the gels were prepared in different concentration
305 using different solvents in 7 mL glass *via*ls. The obtained gels were transferred on to the center of
306 the plate of the rheometer using a spatula. The strain sweep measurements were performed to
307 estimate the strain at a constant stress of 10 Pa. Next, frequency sweep measurements and time
308 sweep measurements were performed in the range 0.1 to 4000 Pa. SEM images were obtained on
309 a Hitachi S-5200 field emission scanning microscope. The samples were prepared by applying
310 directly to silicon wafer chips (Agar Scientific) using a stick. Then the samples were kept in
311 vacuum for slow evaporation of solvents. All three samples were coated with 2 nm of Pt and were
312 imaged at 3 KeV and 0.34 nA.
313
314 ***Characterization of gelators***
315 See ESI for details of gelator synthesis.

316 *Gelator **G1***: Yield = 0.378 g, 0.46 mmol, 85%, MP > 300 ºC. FT-IR: 3320 (N–H), 1692 (C=O),
317 1650 ($N–H_{bend}$) cm^{-1}; ^{1}H-NMR (DMSO-d_6, 400MHz) δ: 0.75 (t, J = 7.6 Hz, 6H, -CH_3) 1.10 (t, J
318 = 8.0 Hz, 12H, -CH_3), 1.75-1.87 (m, 4H, -CH_2), 2.08–2.19 (m, 4H, -CH_2), 2.31–2.46 (m, 4H, -

CH_2) 2.51–2.55 (m, 8H, -CH_2), 3.85 (s, 2H, -CH_2), 6.99 (s, 4H, H-Ph), 7.16 (d, *J* = 8.0 Hz, 4H, H-Ph), 7.43 (d, *J* = 8.0 Hz, 4H, H-Ph), 7.56 (s, 2H, NH), 8.82 (s, 2H, NH), 10.83 (s, 2H, NH).$^{13}C\{^1H\}$-NMR (DMSO-d_6, 100 MHz): δ 176.3, 173.2, 154.3, 142.3, 140.1, 139.7, 132.6, 132.2, 127.0, 126.7, 118.2, 50.0, 32.6, 29.5, 26.4, 24.9, 15.1 and 9.3 ppm. MALDI-TOF MS calc. for M+H 828.02, experimental 828.00. Elemental analysis: Calc. (%) C, 71.20; H, 7.07; N, 10.03; found. (%) C, 71.18; H, 7.11; and N, 10.03.

Gelator ***G2***: Yield= 0.346 g, 0.48 mmol, 90%, MP > 300 ºC. FTIR: 3337 (N–H), 1691 (C=O), 1650 (N–$H_{bending}$) cm^{-1}; ^{1}H-NMR (DMSO-d_6, 400MHz) δ: 0.75 (t, *J* = 7.4 Hz, 6H, -CH_3), 1.77–1.84 (m, 4H, -CH_2), 2.09-2.17 (m, 4H, -CH_2), 2.31–2.47 (m, 4H, -CH_2), 3.81 (s, 2H, -CH_2), 7.11 (d, *J* = 8.0 Hz, 4H, H-Ph), 7.18 (d, *J* = 8.0 Hz, 4H, H-Ph), 7.34 (d, *J* = 8.0 Hz, 4H, H-Ph), 7.43 (d, *J* = 8.0 Hz, 4H, H-Ph), 8.57 (s, 2H, NH), 8.65 (s, 2H, NH), 10.83 (s, 2H, NH). $^{13}C\{^1H\}$-NMR: (DMSO-d_6, 100 MHz): δ176.3, 173.2, 152.9, 139.1, 137.9, 135.5, 133.1, 129.3, 127.1, 118.84, 118.8, 50.1, 32.6, 29.6, 26.4, and 9.3. MS calculated for M+2H is 357.16, experimental 357.39. Elemental analysis: Calc. (%) C, 68.89; H, 5.92; N, 11.76, found (%): C, 68.29; H, 5.81; and N, 11.65.

Gelator ***G3***: Yield= 0.329 g, 0.47 mmol, 87%, MP > 300 ºC. FT-IR: 3341 (N–H), 1695 (C=O), 1641 (N–$H_{bending}$) cm^{-1}. ^{1}H-NMR (DMSO-d_6, 400MHz) δ: 0.74 (t, *J* = 8.0 Hz, 6H, -CH_3), 1.59 (s, 12H, -CH_3), 1.77–1.82 (m, 4H, -CH_2), 2.06–2.16 (m, 4H, -CH_2), 2.28–2.43 (m, 4H, -CH_2), 6.54 (s, 2H, NH), 7.10 (d, *J* = 8 Hz, 4H, H-Ph), 7.23 (s, 4H, H-Ph), 7.31 (d, *J* = 8.0 Hz, 4H, H-Ph), 8.45 (s, 2H, NH), 10.81 (s, 2H, NH).$^{13}C\{^1H\}$-NMR: (DMSO-d_6, 100 MHz): δ 176.3, 173.2, 154.8, 148.3, 139.9, 132.2, 128.0, 126.9, 122.9, 121.7, 118.1, 55.0, 50.0, 46.1, 32.6, 30.2, 29.5, 26.4, 12.1,

and 9.3. MS calculated for M+H is 709.36, experimental 709.55. Elemental analysis: Calc. (%): C, 67.78; H, 6.83; N, 11.86; found (%): C, 67.39; H, 6.62; and N, 11.56

Gel Screening

Gel screening was carried out at a concentration of 2 % (w/v). Samples were dissolved in 0.5 mL of the relevant solvent through gentle heating close to the boiling temperature followed by sonication for 1 min. Gels formation was generally observed within a few minutes but in some case, it requires several hours.

Solution and Gel Phase Recrystallization

Solution crystallizations were performed by the heating of a saturated solution of either BAR or THL until completely dissolved. The solutions were left to cool slowly in a heating block. These were carried out in parallel with gel-phase crystallizations under the same conditions, but in which the heated solution was used to dissolve the gelator. Then the solutions were also left to cool slowly in the heating blocks. Typically gels formed in a few minutes and crystals formed over a matter of hours or days.

Crystal Form Characterisation

Crystals obtained from the solution and gel phase crystallisation experiments were characterized using single crystal x-ray diffraction, XRPD, DSC and microscopic technique.

Supporting Information

Further gelator characterization as well as FT-IR, rheological and XPRD data and Hirshfeld surface analysis available in the electronic supporting information.

Acknowledgements

We thank Dr Dmitry S. Yufit and Andrei S. Batsanov for help with unit cell determinations. We are grateful to the Engineering and Physical Sciences Research Council (EP/R013373/1) and Science Engineering and Research Board, India (CRG/2019/004946) for funding and Commonwealth Scholarships Commission for a Split-Site Doctoral Fellowship (to BS). The authors declare no competing financial interest.

References

(1) Osada, Y.; Khokhlov, A. R. *Polymer Gels and Networks*; Marcel Dekker, 2002.

(2) Terech, P.; Weiss, R. G. Low Molecular Mass Gelators of Organic Liquids and the Properties of Their Gels. *Chem. Rev.* **1997**, *97*, 3133–3160.

(3) Steed, J. W. Supramolecular Gel Chemistry: Developments over the Last Decade. *Chem. Commun.* **2011**, *47*, 1379–1383.

(4) Steed, J. W. Anion-Tuned Supramolecular Gels: A Natural Evolution from Urea Supramolecular Chemistry. *Chem. Soc. Rev.* **2010**, *39*, 3686–3699.

(5) Sangeetha, N. M.; Maitra, U. Supramolecular Gels: Functions and Uses. *Chem. Soc. Rev.* **2005**, *34*, 821–836.

(6) Das, D.; Kar, T.; Das, P. K. Gel-Nanocomposites: Materials with Promising Applications. *Soft Matter* **2012**, *8*, 2348–2365.

(7) Miao, R.; Peng, J.; Fang, Y. Molecular Gels as Intermediates in the Synthesis of Porous Materials and Fluorescent Films: Concepts and Applications. *Langmuir* **2017**, *33*, 10419–

10428.

(8) Babu, S. S.; Praveen, V. K.; Ajayaghosh, A. Functional π-Gelators and Their Applications. *Chem. Rev.* **2014**, *114*, 1973–2129.

(9) Hirst, A. R.; Escuder, B.; Miravet, J. F.; Smith, D. K. High-Tech Applications of Self-Assembling Supramolecular Nanostructured Gel-Phase Materials: From Regenerative Medicine to Electronic Devices. *Angew. Chem. Int. Ed.* **2008**, *47*, 8002–8018.

(10) Serban, B.; Stipe, K.; Alverson, J.; Johnston, E.; Priestley, N.; Serban, M. A Controlled Antibiotic Release System for the Development of Single-Application Otitis Externa Therapeutics. *Gels* **2017**, *3*, 19.

(11) Foster, J. A.; Piepenbrock, M. O. M.; Lloyd, G. O.; Clarke, N.; Howard, J. A. K.; Steed, J. W. Anion-Switchable Supramolecular Gels for Controlling Pharmaceutical Crystal Growth. *Nat. Chem.* **2010**, *2*, 1037–1043.

(12) Dastidar, P. Supramolecular Gelling Agents: Can They Be Designed? *Chem. Soc. Rev.* **2008**, *37*, 2699–2715.

(13) Hirst, A. R., Coates, I. A., Boucheteau, T. R., Miravet, J. F., Escuder, B., Castelletto, V., Hamley, I. W., and Smith, D. K. Low-Molecular-Weight Gelators: Elucidating the Principles of Gelation Based on Gelator Solubility and a Cooperative Self-Assembly Model. *J. Am. Chem. Soc.* **2008**, *130*, 9113–9121.

(14) Zhu, G.; Dordick, J. S. Solvent Effect on Organogel Formation by Low Molecular Weight Molecules. *Chem. Mater.* **2006**, *18*, 5988–5995.

(15) Mulvee, M.; Vasiljevic, N.; Mann, S.; Patil, A. J. Construction of Supramolecular Hydrogels Using Photo-Generated Nitric Oxide Radicals. *Soft Matter* **2018**, *14*, 5950–5954.

(16) Foster, J. A., Damodaran, K. K., Maurin, A., Day, G. M., Thompson, H. P., Cameron, G.

J., Bernal, J. C., and Steed, J. W. Pharmaceutical Polymorph Control in a Drug-Mimetic Supramolecular Gel. *Chem. Sci.* **2016**, *8*, 78–84.

(17) Kumar, D. K.; Steed, J. W. Supramolecular Gel Phase Crystallization: Orthogonal Self-Assembly under Non-Equilibrium Conditions. *Chem. Soc. Rev.* **2014**, *43*, 2080–2088.

(18) Llinàs, A.; Goodman, J. M. Polymorph control: past, present and future. *Drug Discov. Today.* **2008**, *13*, 198−210.

(19) Bora, P.; Saikia, B.; Sarma, B. Oriented Crystallization on Organic Monolayers to Control Concomitant Polymorphism. *Chem. Eur. J.* **2020**, *26*, 699–710.

(20) Su, C. S.; Liao, C. Y.; Jheng, W. De. Particle Size Control and Crystal Habit Modification of Phenacetin Using Ultrasonic Crystallization. *Chem. Eng. Technol.* **2015**, *38*, 181–186.

(21) Trask, A. V. An Overview of Pharmaceutical Cocrystals as Intellectual Property. *Mol. Pharm.* **2007**, *4*, 301–309.

(22) Sugiyama, T.; Masuhara, H. Laser-Induced Crystallization and Crystal Growth. *Chem. Asian J.* **2011**, *6*, 2878–2889.

(23) Chen, J.; Sarma, B.; Evans, J. M. B.; Myerson, A. S. Pharmaceutical Crystallization. *Cryst. Growth Des.* **2011**, *11*, 887–895.

(24) Tyler, A. R.; Ragbirsingh, R.; McMonagle, C. J.; Waddell, P. G.; Heaps, S. E.; Steed, J. W.; Thaw, P.; Hall, M. J.; Probert, M. R. Encapsulated Nanodroplet Crystallization of Organic-Soluble Small Molecules. *Chem* **2020**, *6*, 1755–1765.

(25) Shtukenberg, A. G.; Ward, M. D.; Kahr, B. Crystal Growth with Macromolecular Additives. *Chem. Rev.* **2017**, *117*, 14042–14090.

(26) Lévesque, A.; Maris, T.; Wuest, J. D. ROY Reclaims Its Crown: New Ways To Increase Polymorphic Diversity. *J. Am. Chem. Soc.* **2020**. *142*, 11873–11883.

(27) Zhang, K.; Fellah, N.; Shtukenberg, A. G.; Fu, X.; Hu, C.; Ward, M. D. Discovery of New Polymorphs of the Tuberculosis Drug Isoniazid. *CrystEngComm* **2020**, *22*, 2705–2708.

(28) Duffus, C.; Camp, P. J.; Alexander, A. J. Spatial Control of Crystal Nucleation in Agarose Gel. *J. Am. Chem. Soc.* **2009**, *131*, 11676–11677.

(29) Diao, Y.; Whaley, K. E.; Helgeson, M. E.; Woldeyes, M. A.; Doyle, P. S.; Myerson, A. S.; Hatton, T. A.; Trout, B. L. Gel-Induced Selective Crystallization of Polymorphs. *J. Am. Chem. Soc.* **2012**, *134*, 673–684.

(30) Iuzzolino, L.; McCabe, P.; Price, S. L.; Brandenburg, J. G. Crystal Structure Prediction of Flexible Pharmaceutical-like Molecules: Density Functional Tight-Binding as an Intermediate Optimisation Method and for Free Energy Estimation. *Faraday Discuss.* **2018**, *211*, 275–296.

(31) Schneider, E.; Vogt, L.; Tuckerman, M. E.; IUCr. Exploring Polymorphism of Benzene and Naphthalene with Free Energy Based Enhanced Molecular Dynamics. *Acta Crystallogr. Sect. B Struct. Sci. Cryst. Eng. Mater.* **2016**, *72*, 542–550.

(32) Thompson, H. P. G.; Day, G. M. Which Conformations Make Stable Crystal Structures? Mapping Crystalline Molecular Geometries to the Conformational Energy Landscape. *Chem. Sci.* **2014**, *5*, 3173–3182.

(33) Dawn, A.; Andrew, K. S.; Yufit, D. S.; Hong, Y.; Reddy, J. P.; Jones, C. D.; Aguilar, J. A.; Steed, J. W. Supramolecular Gel Control of Cisplatin Crystallization: Identification of a New Solvate Form Using a Cisplatin-Mimetic Gelator. *Cryst. Growth Des.* **2015**, *15*, 4591–4599.

(34) Tokunaga, E.; Yamamoto, T.; Ito, E.; Shibata, N. Understanding the Thalidomide Chirality in Biological Processes by the Self-Disproportionation of Enantiomers. *Sci. Rep.* **2018**, *8*,

17131.

(35) Reepmeyer, J. C.; Rhodes, M. O.; Cox, D. C.; Silverton, J. V. Characterization and Crystal Structure of Two Polymorphic Forms of Racemic Thalidomide. *J. Chem. Soc. Perkin Trans. 2* **1994**, *0*, 2063.

(36) Zencirci, N.; Griesser, U. J.; Gelbrich, T.; Apperley, D. C.; Harris, R. K. Crystal Polymorphs of Barbital: News about a Classic Polymorphic System. *Mol. Pharm.* **2014**, *11*, 338–350.

(37) MacDonald, J. C.; Biyikli, K.; Zugic, B.; Ebersole, G.; Allor, J. Nucleation and Growth of Polymorphs of Barbital on Chemically Modified Surfaces in Microfluidic Channels. *Mater. Res. Soc. Symp. Proc.* **2005**, *901*, 110–116.

(38) Bernstein, J.; Davey, R. J.; Henck, J. O. Concomitant Polymorphs. *Angew. Chem. Int. Ed.* **1999**, *38*, 3440–3461.

(39) Munshi, P.; Venugopala, K. N.; Jayashree, B. S.; Guru Row, T. N. Concomitant Polymorphism in 3-Acetylcoumarin: Role of Weak C−H···O and C−H···π Interactions. *Cryst. Growth Des.* **2004**, *4*, 1105–1107.

(40) Jiang, S.; Ter Horst, J. H.; Jansens, P. J. Concomitant Polymorphism of O-Aminobenzoic Acid in Antisolvent Crystallization. *Cryst. Growth Des.* **2008**, *8*, 37–43.

(41) Baral, A.; Basak, S.; Basu, K.; Dehsorkhi, A.; Hamley, I. W.; Banerjee, A. Time-Dependent Gel to Gel Transformation of a Peptide Based Supramolecular Gelator. *Soft Matter* **2015**, *11*, 4944–4951.

(42) Castilla, A. M.; Wallace, M.; Mears, L. L. E.; Draper, E. R.; Doutch, J.; Rogers, S.; Adams, D. J. On the Syneresis of an OPV Functionalised Dipeptide Hydrogel. *Soft Matter* **2016**, *12*, 7848–7854.

(43) Torres-Moya, I.; Saikia, B.; Prieto, P.; Carrillo, J. R.; Steed, J. W. High Thermal Stability,

PH Responsive Organogels of 2H-Benzo[d]1,2,3-Triazole Derivatives as Pharmaceutical Crystallization Media. *CrystEngComm* **2019**, *21*, 2135–2143.

(44) Zuidema, J. M.; Rivet, C. J.; Gilbert, R. J.; Morrison, F. A. A Protocol for Rheological Characterization of Hydrogels for Tissue Engineering Strategies. *J. Biomed. Mater. Res. Part B Appl. Biomater.* **2014**, *102*, 1063–1073.

(45) Guvendiren, M.; Lu, H. D.; Burdick, J. A. Shear-Thinning Hydrogels for Biomedical Applications. *Soft Matter* **2012**, *8*, 260–272.

(46) Gavezzotti, A.; Filippini, G. Geometry of the Intermolecular X-H.Cntdot..Cntdot..Cntdot.Y (X, Y = N, O) Hydrogen Bond and the Calibration of Empirical Hydrogen-Bond Potentials. *J. Phys. Chem.* **1994**, *98*, 4831–4837.

(47) Gavezzotti, A. Are Crystal Structures Predictable? *Acc. Chem. Res.* **1994**, *27*, 309–314.

(48) MacRae, C. F.; Sovago, I.; Cottrell, S. J.; Galek, P. T. A.; McCabe, P.; Pidcock, E.; Platings, M.; Shields, G. P.; Stevens, J. S.; Towler, M.; Wood, P. A. Mercury 4.0: From Visualization to Analysis, Design and Prediction. *J. Appl. Crystallogr.* **2020**, *53*, 226–235.

(49) Groom, C. R.; Bruno, I. J.; Lightfoot, M. P.; Ward, S. C. The Cambridge Structural Database. *Acta Crystallogr. Sect. B Struct. Sci. Cryst. Eng. Mater.* **2016**, *72*, 171–179.

(50) Cayuela, A.; Soriano, M. L.; Kennedy, S. R.; Steed, J. W.; Valcárcel, M. Fluorescent Carbon Quantum Dot Hydrogels for Direct Determination of Silver Ions. *Talanta* **2016**, *151*, 100–105.

(51) Spackman, M. A.; McKinnon, J. J. Fingerprinting Intermolecular Interactions in Molecular Crystals. *CrystEngComm* **2002**, *4*, 378–392.

(52) Velásquez-González, O.; Campos-Escamilla, C.; Flores-Ibarra, A.; Esturau-Escofet, N.; Arreguin-Espinosa, R.; Stojanoff, V.; Cuéllar-Cruz, M.; Moreno, A. Crystal Growth in Gels

from the Mechanisms of Crystal Growth to Control of Polymorphism: New Trends on Theoretical and Experimental Aspects. *Crystals* **2019**, *9*, 443.

Table of Contents Graphic